Magnetically Driven Suppression of Nematic Order in an Iron-Based Superconductor

J. M. Allred – Argonne National Laboratory, Illinois
et al.

Citation of published version:
Avci, S., et al. (2013): Magnetically Driven Suppression of Nematic Order in an Iron-Based Superconductor. *Nature Communications*, 5.
DOI: https://doi.org/10.1038/ncomms4845

nature COMMUNICATIONS

ARTICLE

Received 10 Mar 2013 | Accepted 8 Apr 2014 | Published 22 May 2014

DOI: 10.1038/ncomms4845

Magnetically driven suppression of nematic order in an iron-based superconductor

S. Avci[1,†], O. Chmaissem[1,2], J.M. Allred[1], S. Rosenkranz[1], I. Eremin[3], A.V. Chubukov[4], D.E. Bugaris[1], D.Y. Chung[1], M.G. Kanatzidis[1,5], J.-P Castellan[1], J.A. Schlueter[1], H. Claus[1], D.D. Khalyavin[6], P. Manuel[6], A. Daoud-Aladine[6] & R. Osborn[1]

A theory of superconductivity in the iron-based materials requires an understanding of the phase diagram of the normal state. In these compounds, superconductivity emerges when stripe spin density wave (SDW) order is suppressed by doping, pressure or atomic disorder. This magnetic order is often pre-empted by nematic order, whose origin is yet to be resolved. One scenario is that nematic order is driven by orbital ordering of the iron 3*d* electrons that triggers stripe SDW order. Another is that magnetic interactions produce a spin-nematic phase, which then induces orbital order. Here we report the observation by neutron powder diffraction of an additional fourfold-symmetric phase in $Ba_{1-x}Na_xFe_2As_2$ close to the suppression of SDW order, which is consistent with the predictions of magnetically driven models of nematic order.

[1] Materials Science Division, Argonne National Laboratory, Argonne, Illinois 60439-4845, USA. [2] Department of Physics, Northern Illinois University, DeKalb, Illinois 60115, USA. [3] Institut für Theoretische Physik III, Ruhr-Universität Bochum, 44801 Bochum, Germany. [4] Department of Physics, University of Wisconsin-Madison, Madison, Wisconsin 53706, USA. [5] Department of Chemistry, Northwestern University, Evanston, Illinois 60208-3113, USA. [6] ISIS Pulsed Neutron and Muon Facility, Rutherford Appleton Laboratory, Chilton, OX11 0QX, UK. † Present address: Department of Materials Science and Engineering, Afyon Kocatepe University, 03200 Afyon, Turkey. Correspondence and requests for materials should be addressed to R.O. (email: ROsborn@anl.gov).

There have been extensive investigations of the phase diagrams of the various iron arsenide and chalcogenide structures that display high temperature superconductivity with critical temperatures up to 55 K[1–4]. In common with other unconventional superconductors, such as the copper oxides, heavy fermions and organic charge-transfer salts, superconductivity is induced by suppressing a magnetically ordered phase, which generates a high density of magnetic fluctuations that could theoretically bind the Cooper pairs. Whether this is responsible for the high transition temperatures has not been conclusively established, but it makes the origin of the magnetic interactions an important issue to be resolved[5,6].

In nearly all the iron arsenides and chalcogenides, the iron atoms form a square planar net and the magnetic order consists of ferromagnetic stripes along one iron–iron bond direction that are antiferromagnetically aligned along the orthogonal iron–iron bond[6,7]. These systems are metallic and the Fermi surfaces, which are formed by the iron 3*d* electrons, are nearly cylindrical with hole pockets at the centre of the Brillouin zone and electron pockets at the zone boundaries, all of similar size. In such an electronic structure, interactions between electrons near the two sets of pockets give rise to a spin density wave (SDW) order at the wave vector connecting them[8]. This itinerant picture is consistent with the wave vector of the observed antiferromagnetism, angle resolved photoemission (ARPES) measurements of the electronic structure[9,10] and the evolution of the dynamic magnetic susceptibility with carrier concentration[11–13].

However, any theory of the magnetic order also has to explain the structural transition that occurs at a temperature either just above or coincident with the SDW transition and lowers the symmetry from tetragonal (C_4) to orthorhombic (C_2). This is often referred to as nematic order, and the relation between nematicity, magnetic order and superconductivity has become one of the central questions in the iron-based superconductors[14,15].

At present, there are two scenarios for the development of nematic order and its relation to SDW order. In the first, the structural order is unrelated to magnetism and is driven by orbital ordering as the primary instability. The orbital ordering induces magnetic anisotropy and triggers the magnetic transition at a lower temperature by renormalizing the exchange constants[16–18]. This scenario is largely phenomenological, but there have been recent efforts to develop a microscopic basis[19].

In the second scenario, the structural order is driven by magnetic fluctuations, associated with the fact that striped SDW order can be along the *x*-axis (ordered momentum is $\mathbf{Q}_X=(0,\pi)$) or along the *y*-axis (ordered momentum is $\mathbf{Q}_Y=(\pi,0)$). Theory predicts that the Z_2 symmetry between the *X* and *Y* directions can be broken above the true SDW ordering temperature that breaks $O(3)$ spin symmetry, that is, the system distinguishes between $\mathbf{Q}_X$ and $\mathbf{Q}_Y$ without breaking time reversal symmetry[20]. The order parameter of this 'Ising-spin-nematic state' couples linearly to the lattice, inducing both structural and orbital order. The magnetic scenario has been developed for itinerant[8,20] and localized[21–24] electrons, and the phase diagrams are rather similar in the two approaches. Below we use the fact that the systems we study are metals and use an itinerant approach.

Many of the observable properties are identical in both the orbital and magnetic scenarios, hindering a determination of the origin of nematicity. In the following, we report the discovery of a new magnetic phase in hole-doped $Ba_{1-x}Na_xFe_2As_2$ (refs 25,26) at doping levels close to the suppression of magnetic order. This second phase, which occurs at temperatures below the conventional C_2 transition, restores C_4 rotational symmetry, indicating that the SDW order combines $\mathbf{Q}_X$ *and* $\mathbf{Q}_Y$ with equal weights. Such a second transition is highly unlikely in an orbital scenario because the breaking of symmetry of $\mathbf{Q}_X$ and $\mathbf{Q}_Y$ is a precondition for a magnetic transition to occur. However, it is known that such a phase is a possible solution of itinerant magnetic models for certain combinations of electronic interactions and/or Fermi surface geometries[8,27–29]. By going beyond our earlier Ginzburg-Landau analysis, we now show that the phase diagram is much richer than previously thought and that the C_4 phase becomes energetically favourable at higher doping levels, particularly in the range of phase coexistence with superconductivity[29]. We therefore view the observation of the transition to an SDW state, which does not break the symmetry between $\mathbf{Q}_X$ and $\mathbf{Q}_Y$, as a strong indication that the nematic order is of magnetic origin.

A magnetically driven C_4 phase also provides a natural explanation for the new phase observed in transport measurements in $Ba_{1-x}K_xFe_2As_2$ under external pressure[30] and may explain anomalous diffraction results in $Ba(Fe_{1-x}Mn_x)_2As_2$ (ref. 31), so it is probably present in other iron-based superconductors, although our calculations show that its stability is highly sensitive to details of the electronic structure.

In the following, we describe the experimental evidence for a re-entrant C_4 phase in neutron and x-ray diffraction data on $Ba_{1-x}Na_xFe_2As_2$ for $x\geq 0.24$. We then summarize the results of theoretical calculations showing that such a phase is consistent with magnetically driven nematic order.

Results

Experiment. We have conducted a detailed survey of the phase diagram of $Ba_{1-x}Na_xFe_2As_2$ using neutron and x-ray powder diffraction[25], following our recent investigation of the potassium-doped compounds[32]. In both the K-doped and Na-doped series, the addition of the alkali metal dopes holes into iron *d*-bands and reduces the transition temperature into the stripe phase from 139 K, in the parent compound $BaFe_2As_2$, to 0 at $x\sim 0.25-0.3$. One unusual feature of both series is that the antiferromagnetic and orthorhombic transitions are coincident and first-order over the entire phase diagram[33], an observation that is quite unambiguous since both order parameters are determined from the same neutron powder diffraction measurement.

Details of the synthesis and characterization of the polycrystalline samples and the powder diffraction measurements are given in the Methods section. We provide a comparison of the sample stoichiometries with earlier reports in Supplementary Note 1.

The only region of the sodium series where there are significant departures from the conventional behaviour observed in many iron-based superconductors is at $0.24\leq x\leq 0.28$ close to the suppression of the AF/O order. These compounds are all in the region where superconductivity coexists with magnetic order at low temperature. The results are summarized in Fig. 1, where diffractograms are shown for three Bragg reflections at $(h,k,l)=(112)$, $\left(\frac{1}{2}\frac{1}{2}1\right)$ and $\left(\frac{1}{2}\frac{1}{2}3\right)$, respectively, using tetragonal reciprocal lattice indices. The (112) reflection is a nuclear Bragg peak that splits when the symmetry is lowered to orthorhombic, while the other two reflections are magnetic Bragg peaks.

At $x=0.24$ and 0.26, the transition into the C_2 (*Fmmm*) phase at $T_N\sim 70$–90 K is clearly evident. However, at $T_r\sim 40$–50 K, there is a second phase transition, not seen at $x=0.22$ (not shown), at which the orthorhombic splitting collapses and tetragonal C_4 (*I*4/*mmm*) symmetry is restored. The $\left(\frac{1}{2}\frac{1}{2}3\right)$ reflection, which shows the onset of stripe SDW order at T_N, weakens in intensity in the C_4 phase, whereas the $\left(\frac{1}{2}\frac{1}{2}1\right)$ reflection strengthens considerably. This indicates that there is a strong spin reorientation with respect to the stripe SDW order when tetragonal symmetry is restored at T_r. It was not possible to obtain an unambiguous refinement of the C_4 magnetic structure;

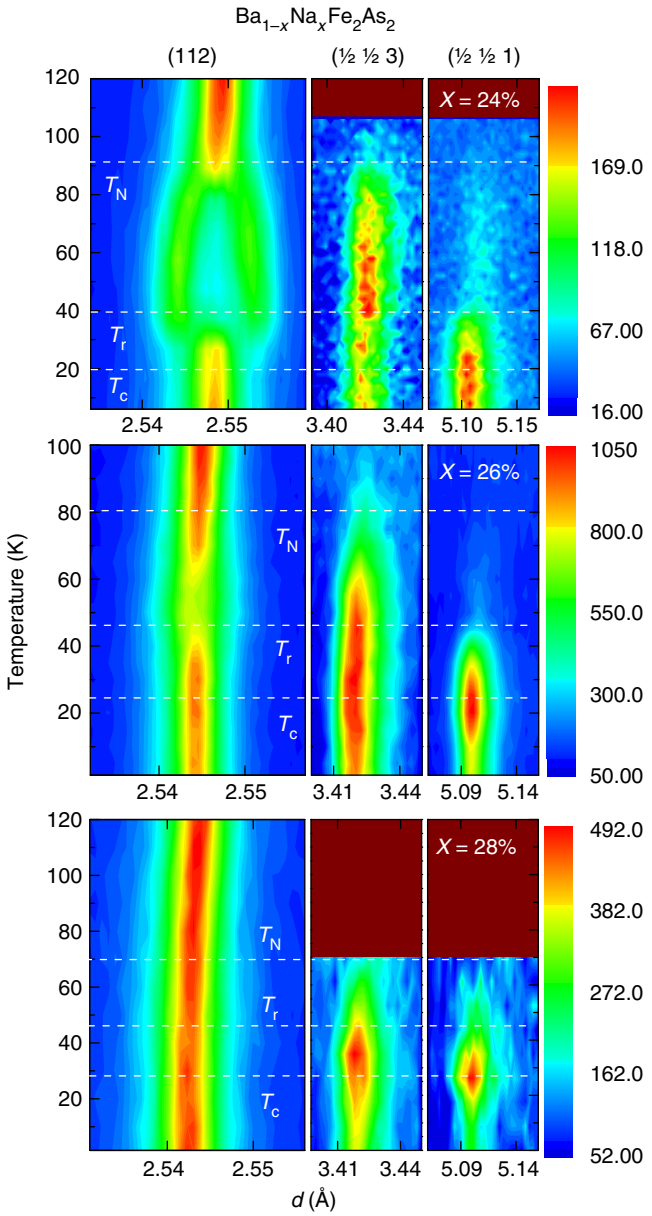

Figure 1 | Temperature dependence of powder neutron diffraction from $Ba_{1-x}Na_xFe_2As_2$. The first diffractogram is of HRPD data from the (112) Bragg peak (using tetragonal indices), which shows the orthorhombic transition at T_N and the re-entrant tetragonal transition at T_r in $x=0.24$ and 0.26. The symmetry is tetragonal at all temperatures in $x=0.28$. The other two diffractograms are of Wish data from magnetic Bragg peaks. The $(\frac{1}{2}\frac{1}{2}3)$ data show the onset of stripe SDW order at T_N. The $(\frac{1}{2}\frac{1}{2}1)$ data show the onset of the C_4 SDW order at T_r. The absolute intensities are arbitrary, but, to display all the plots on the same colour scale, the $(\frac{1}{2}\frac{1}{2}3)$ intensities have been multiplied by factors of 208, 200 and 144, and the $(\frac{1}{2}\frac{1}{2}1)$ by factors of 30, 20 and 60, for $x=0.24$, 0.26 and 0.28, respectively. The magnetic Bragg peaks show a significant reduction of intensity below the superconducting transition at T_c, indicating the phase competition between magnetism and superconductivity.

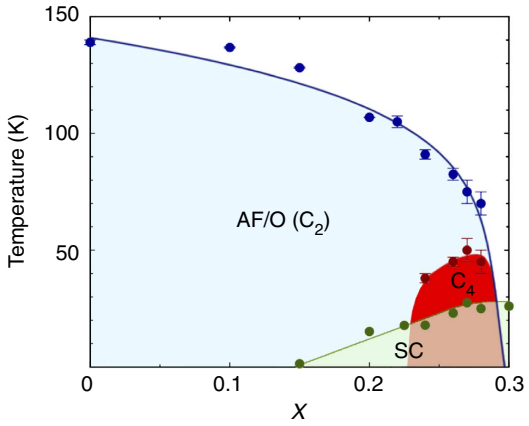

Figure 2 | Phase diagram of $Ba_{1-x}Na_xFe_2As_2$. The blue points are the coincident antiferromagnetic and orthorhombic transition temperatures, T_N, into the C_2 phase, and the red points are the observed transition temperatures, T_r, into the C_4 phase, all measured by neutron diffraction. The green points are the superconducting transition temperatures, T_c, determined from magnetization data. The error bars represent the temperature interval in the neutron diffraction measurements.

hence, we cannot determine whether the reorientation is in-plane or out-of-plane. A full solution will require measurements on single crystals.

At $x=0.27$ (not shown) and 0.28, the temperature variation of the $(\frac{1}{2}\frac{1}{2}3)$ and $(\frac{1}{2}\frac{1}{2}1)$ reflections show evidence of the same two magnetic transitions at T_N and T_r, although the orthorhombic splitting is too weak to be detected in the intermediate phase even on a high-resolution diffractometer like HRPD.

These observations are summarized in the phase diagram of Fig. 2, which shows that the new phase is confined to doping levels very close to the suppression of stripe SDW order. At $x=0.24$, the lower transition at T_r is very sharp and appears to be first-order because there is evidence that up to 40% of the sample remains in the C_2 phase below T_r. The C_2 phase fraction is reduced to 20% at $x=0.26$. It is not possible to determine whether there is phase coexistence at higher doping. Further details of the coexistence of C_2 and C_4 phases at $x=0.24$ and 0.26 are provided in Supplementary Note 2.

Figure 1 shows that the C_4 phase competes with the superconductivity because there is a strong suppression of the magnetic peak intensities at temperatures below T_c. This is similar to the phase competition between superconductivity and the C_2 phase seen in the electron-doped superconductors[34], but much stronger than the phase competition observed in the $Ba_{1-x}K_xFe_2As_2$ series[33].

Theory. The itinerant description of magnetism in iron-based superconductors is built on the fact that the hole bands are centred around $\mathbf{Q}_\Gamma=(0, 0)$ and the electron bands are centred at $\mathbf{Q}_X=(\pi, 0)$ and $\mathbf{Q}_Y=(0, \pi)$, respectively (Fig. 3a). The spin susceptibility is logarithmically enhanced at momenta connecting the hole and electron pockets, and SDW order develops even if the interaction is weak. The SDW order parameter is in general a combination of the two vector components $\mathbf{\Delta}_X$ and $\mathbf{\Delta}_Y$ with momenta $(\pi, 0)$ and $(0, \pi)$, respectively. For a model of perfect Fermi surface nesting (circular hole and electron pockets of equal radii) and only electron–hole interactions, SDW order determines $|\mathbf{\Delta}_X|^2+|\mathbf{\Delta}_Y|^2$ but not the relative magnitudes and directions of $\mathbf{\Delta}_X$ and $\mathbf{\Delta}_Y$. Away from perfect nesting, the ellipticity of the electron pockets and interactions between the electron bands break the degeneracy and lower the symmetry of the SDW order. Near T_N, an analysis within a Ginzburg-Landau expansion in powers of $\mathbf{\Delta}_X$ and $\mathbf{\Delta}_Y$ shows that fourth-order terms select stripe magnetic order with either $\mathbf{\Delta}_X\neq0$, $\mathbf{\Delta}_Y=0$ or $\mathbf{\Delta}_Y\neq0$, $\mathbf{\Delta}_X=0$ (refs 8,20). Such an order simultaneously reduces the lattice C_4 symmetry

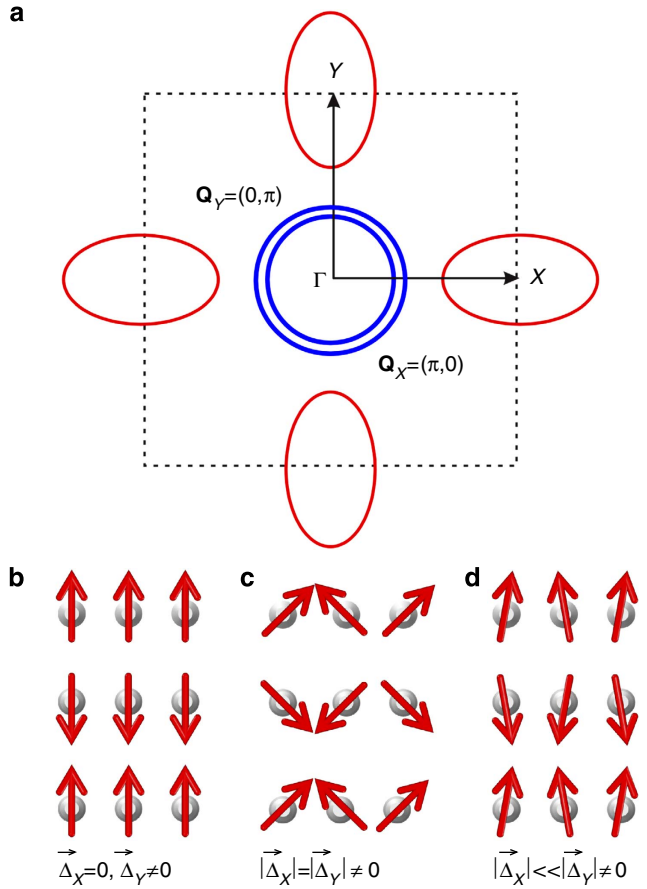

Figure 3 | Spin-nematic models of magnetic order. (**a**) The band-structure with two circular hole pockets at Γ and two electron pockets at *X* and *Y*, using the unfolded Brillouin zone with one Fe atom per unit cell. The arrows refer to two equivalent nesting wave vectors $\mathbf{Q}_X=(\pi, 0)$ and $\mathbf{Q}_Y=(0, \pi)$. (**b**–**d**) Possible magnetic ground states of the Fe-lattice: (**b**) the C_2 antiferromagnetic stripe phase with $\Delta_X=0$ and $\Delta_Y\neq 0$; (**c**) a C_4 magnetic state, in which $|\Delta_X|=|\Delta_Y|\neq 0$, that is compatible with tetragonal lattice symmetry (this is one of several possible solutions of the C_4 magnetic structures); (**d**) magnetic order in which $|\Delta_X| \ll |\Delta_Y|\neq 0$. Note that the Néel transition at low temperatures, T_r, from phase (**b**) to phase (**c**) is first order, while the transition from phase (**b**) to phase (**d**) is second order, in which an additional small component of Δ_X appears below T_r. Our experiments are more compatible with scenario (**c**).

down to C_2. The order parameter in the stripe phase is shown schematically in Fig. 3b.

An issue that has not been discussed in detail until now is whether another magnetic ground state, in which both $\mathbf{\Delta}_X$ and $\mathbf{\Delta}_Y$ are non-zero, may appear at a lower temperature, as a result of non-linear effects. This might happen either via a first-order transition, in which case the most likely outcome is the state in which $|\Delta_X|=|\Delta_Y|$ (see Fig. 3c), or via a second-order transition, in which case the second order parameter appears continuously and likely remains relatively small down to $T=0$.

To check for a potential second SDW transition, we needed to go beyond the previous Ginzburg-Landau analysis; hence, we solved non-linear coupled mean-field equations for Δ_X and Δ_Y over the entire temperature range and analysed which solution minimizes the free energy. This has revealed new features in the phase diagram not previously identified. In particular, we find that SDW order with $\mathbf{\Delta}_X=\mathbf{\Delta}_Y$, which breaks $O(3)$ spin symmetry but preserves lattice C_4 symmetry, does emerge at low T, as the mismatch in hole and electron pocket sizes grows.

We obtained this result by analysing the minimal three-band model with one hole and two electron pockets. For simplicity, we considered parabolic dispersions with

$$\xi_{\Gamma,\mathbf{k}} = \varepsilon_0 - \frac{k^2}{2m} - \mu \quad (1)$$

$$\xi_{X,\mathbf{k}+\mathbf{Q}_X} = -\varepsilon_0 + \frac{k_x^2}{2m_x} + \frac{k_y^2}{2m_y} - \mu \quad (2)$$

$$\xi_{Y,\mathbf{k}+\mathbf{Q}_Y} = -\varepsilon_0 + \frac{k_x^2}{2m_y} + \frac{k_y^2}{2m_x} - \mu \quad (3)$$

where m_i are band masses, ε_0 is the offset energy and μ is the chemical potential.

The non-interacting Hamiltonian takes the form

$$\mathcal{H}_0 = \sum_{i,\mathbf{k}} \xi_{i,\mathbf{k}} c^{\dagger}_{i,\mathbf{k}\alpha} c_{i,\mathbf{k}\alpha} \quad (4)$$

where $i=1$–3 label the bands, the summation over repeated spin indices α is assumed, and we shift the momenta of the fermions near the *X* and *Y* Fermi pockets by $\mathbf{Q}_X$ and $\mathbf{Q}_Y$, respectively, writing $\xi_{X,\mathbf{k}+\mathbf{Q}_X}=\xi_{2,\mathbf{k}}$, $\xi_{Y,\mathbf{k}+\mathbf{Q}_Y}=\xi_{3,\mathbf{k}}$.

The interaction term in the Hamiltonian $\mathcal{H}_{int}$ contains all symmetry-allowed interactions between low-energy fermions, which include inter- and intra-band scattering processes[35]. We present the explicit form of $\mathcal{H}_{int}$ in the Supplementary Methods. The mean-field equations on $\mathbf{\Delta}_X$ and $\mathbf{\Delta}_Y$ are obtained by introducing $\Delta_X=(1/2N)\sum_k c^{\dagger}_{1,\mathbf{k}\alpha}\vec{\sigma}_{\alpha\beta}c_{2,\mathbf{k}\beta}$ and $\Delta_Y=(1/2N)\sum_k c^{\dagger}_{1,\mathbf{k}\alpha}\vec{\sigma}_{\alpha\beta}c_{3,\mathbf{k}\beta}$ and using them to decouple four-fermion terms into anomalous quadratic terms with inter-band 'hopping', which depends on $\mathbf{\Delta}_X$ and $\mathbf{\Delta}_Y$. We diagonalized the quadratic form, re-expressed $c_{i,\mathbf{k}\alpha}$ in terms of new operators and obtained a set of two coupled self-consistent equations for $\mathbf{\Delta}_X$ and $\mathbf{\Delta}_Y$.

We solved the mean-field equations numerically as a function of two parameters, δ_0 and δ_2 (see Supplementary Methods for details). The parameter $\delta_0=2\mu$ represents the mismatch in chemical potentials of the hole and electron pockets ($\delta_0=0$ when the electron and hole pockets are identical). $\delta_2=\varepsilon_0 m(m_x-m_y)/(2m_x m_y)$ is proportional to the ellipticity of the electron pockets. We focused on the two SDW-ordered states, on the antiferromagnetic stripe state with $\mathbf{\Delta}_X\neq 0$ and $\mathbf{\Delta}_Y=0$, in which C_4-symmetry is reduced to C_2, and the SDW state with $\mathbf{\Delta}_X=\mathbf{\Delta}_Y$, in which C_4-symmetry is preserved. As we said, the two states are degenerate at zero ellipticity and perfect nesting, when $\delta_2=\delta_0=0$. Once the ellipticity becomes non-zero, the stripe state wins immediately below the Néel temperature T_N. The C_4-preserving state (with $\mathbf{\Delta}_X=\mathbf{\Delta}_Y$) is a local maximum and is unstable at $T\leq T_N$.

By solving the equations at lower temperature, we found that, at a finite δ_0, the C_4-preserving state also becomes locally stable below some $T<T_N$, and, at an even lower $T<T_N$, its free energy becomes smaller than that of the stripe phase, that is, at $T=T_r$ the system undergoes a first-order phase transition in which lattice C_4 symmetry gets restored (see Fig. 3c). Because T_N falls as the Fermi surface mismatch δ_0 increases, the new C_4-preserving phase in practice exists only in a narrow region of the phase diagram close to the suppression of SDW order, as observed in Fig. 2. We also analysed a four-pocket model with two hole pockets and found another scenario for a second SDW transition. Namely, the AF stripe order $\mathbf{\Delta}_Y$ initially involves only fermions from a hole pocket, which has higher density of states. Below some $T<T_N$, fermions near the remaining hole pocket and near the electron pocket at *X*, not involved in the initial stripe order,

also produce a SDW instability, and the system gradually develops the second order parameter $|\Delta_X|$, which distorts the stripe AF order. The corresponding low T-spin configuration is shown in Fig. 3d. In this case, however, the C_4 symmetry remains broken at all temperatures. Our experimental data taken as a function of doping are more consistent with a first-order transition and restoration of C_4 symmetry, although it is possible that the second scenario is realized under pressure[30].

Discussion

We have demonstrated the existence of a wholly new magnetic phase that exists at the boundary between superconductivity and stripe magnetism, an observation that has important implications for the origin of magnetic and structural transitions in the iron-based superconductors. It is important to distinguish these new results from previous observations of a re-entrant tetragonal phase in electron-doped compounds, such as $BaFe_{2-x}Co_xAs_2$ (ref. 34). All those transitions were within the superconducting phase and have been shown to result from the competition between superconductivity and stripe SDW order[36,37]. The re-entrant phase that we report here occurs at temperatures that are more than twice as high as T_c and so requires a different explanation. However, there is a similar competition between magnetism and superconductivity in the new phase evident from the partial suppression of the ordered magnetic moment below T_c.

We are unaware of any model of orbital order that would predict a re-entrant non-orbitally ordered phase at lower temperature. However, the prediction of spin-nematic models that a C_4 phase can become degenerate with the C_2 phase only at higher doping when the hole and electron Fermi surfaces are not as well-matched in size, and that the stability of the C_4 phase would be limited to a very narrow region close to the suppression of antiferromagnetism is borne out by the new data.

Our results therefore provide strong evidence for the validity of an itinerant model of nematic order in the iron-based superconductors, in which the orbital reconstruction of the iron 3*d* states is a consequence of magnetic interactions induced by Fermi surface nesting. Whether nematic order, or at least strong nematic fluctuations, is a prerequisite for superconductivity is another challenge to address in the future.

Methods

Sample synthesis. Mixtures of Ba, Na and FeAs were loaded in alumina tubes, sealed in niobium tubes under argon and sealed again in quartz tubes under vacuum. The mixtures were variously subjected to 3–5 firings between 800 and 850 °C for 2–3 days for each firing, except for $Ba_{0.78}Na_{0.22}Fe_2As_2$, which underwent two firings as above, and then was heated for 16 h at 1,000 °C for each of the last two anneals. Between each anneal, the powders were homogenized by grinding in a mortar and pestle. Annealing steps were kept as short as possible, enough to get chemically homogeneous powders while minimizing sodium loss, which is unavoidable. Before the last anneal, a slight amount of NaAs was added to compensate for the loss. The structure and quality of the final black powders were confirmed by x-ray powder diffraction and magnetization measurements. The magnetization curves of the measured samples are shown in Supplementary Fig. 1.

Powder diffraction. The powder diffraction measurements were performed using two beam lines at the ISIS Pulsed Neutron Source, Rutherford Appleton Laboratory, UK: the high-resolution powder diffractometer, HRPD, and the cold-neutron powder diffractometer, Wish. The high resolution available at HRPD was necessary to resolve the weak orthorhombic splitting, while the high flux of Wish was required to measure the weak magnetic reflections. The same samples were used on both diffractometers within a few days of measurement. The results are summarized in the diffractograms (plots of intensity versus *d*-spacing and temperature), shown in Fig. 1, with additional details provided by Supplementary Fig. 2.

References

1. Stewart, G. Superconductivity in iron compounds. *Rev. Mod. Phys.* **83,** 1589–1652 (2011).
2. Paglione, J. & Greene, R. L. High-temperature superconductivity in iron-based materials. *Nat. Phys.* **6,** 645–658 (2010).
3. Johnston, D. C. The puzzle of high temperature superconductivity in layered iron pnictides and chalcogenides. *Adv. Phys.* **59,** 803–1061 (2010).
4. Canfield, P. C. & Bud'ko, S. FeAs-based superconductivity: a case study of the effects of transition metal doping on $BaFe_2As_2$. *Ann. Rev. Cond. Matt. Phys.* **1,** 27–50 (2010).
5. Dai, P., Hu, J. & Dagotto, E. Magnetism and its microscopic origin in iron-based high-temperature superconductors. *Nat. Phys.* **8,** 709–718 (2012).
6. Lumsden, M. D. & Christianson, A. D. Magnetism in Fe-based superconductors. *J. Phys. Condens. Matter* **22,** 203203 (2010).
7. de la Cruz, C. *et al.* Magnetic order close to superconductivity in the iron-based layered $LaO_{1-x}F_xFeAs$ systems. *Nature* **453,** 899–902 (2008).
8. Eremin, I. & Chubukov, A. V. Magnetic degeneracy and hidden metallicity of the spin-density-wave state in ferropnictides. *Phys. Rev. B* **81,** 024511 (2010).
9. Ding, H. *et al.* Observation of Fermi-surface-dependent nodeless superconducting gaps in $Ba_{0.6}K_{0.4}Fe_2As_2$. *EPL* **83,** 47001 (2008).
10. Liu, C. *et al.* K-doping dependence of the Fermi surface of the iron-arsenic $Ba_{1-x}K_xFe_2As_2$ superconductor using angle-resolved photoemission spectroscopy. *Phys. Rev. Lett.* **101,** 177005 (2008).
11. Castellan, J.-P. *et al.* Effect of fermi surface nesting on resonant spin excitations in $Ba_{1-x}K_xFe_2As_2$. *Phys. Rev. Lett.* **107,** 177003 (2011).
12. Lee, C. *et al.* Incommensurate spin fluctuations in hole-overdoped superconductor KFe_2As_2. *Phys. Rev. Lett.* **106,** 067003 (2011).
13. Luo, H. *et al.* Electron doping evolution of the anisotropic spin excitations in $BaFe_{2-x}Ni_xAs_2$. *Phys. Rev. B* **86,** 024508 (2012).
14. Kasahara, S. *et al.* Electronic nematicity above the structural and superconducting transition in $BaFe_2(As_{1-x}P_x)_2$. *Nature* **486,** 382–385 (2012).
15. Fernandes, R. M., Chubukov, A. V. & Schmalian, J. What drives nematic order in iron-based superconductors? *Nat. Phys.* **10,** 97–104 (2014).
16. Krüger, F., Kumar, S., Zaanen, J. & van den Brink, J. Spin-orbital frustrations and anomalous metallic state in iron-pnictide superconductors. *Phys. Rev. B* **79,** 054504 (2009).
17. Lv, W., Wu, J. & Phillips, P. Orbital ordering induces structural phase transition and the resistivity anomaly in iron pnictides. *Phys. Rev. B* **80,** 224506 (2009).
18. Chen, C.-C. *et al.* Orbital order and spontaneous orthorhombicity in iron pnictides. *Phys. Rev. B* **82,** 100504(R) (2010).
19. Inoue, Y., Yamakawa, Y. & Kontani, H. Impurity-induced electronic nematic state and C_2-symmetric nanostructures in iron pnictide superconductors. *Phys. Rev. B* **85,** 224506 (2012).
20. Fernandes, R. M., Chubukov, A. V., Knolle, J., Eremin, I. & Schmalian, J. Preemptive nematic order, pseudogap, and orbital order in the iron pnictides. *Phys. Rev. B* **85,** 024534 (2012).
21. Chandra, P., Coleman, P. & Larkin, A. I. Ising transition in frustrated Heisenberg models. *Phys. Rev. Lett.* **64,** 88–91 (1990).
22. Xu, C., Müller, M. & Sachdev, S. Ising and spin orders in the iron-based superconductors. *Phys. Rev. B* **78,** 020501(R) (2008).
23. Fang, C., Yao, H., Tsai, W.-F., Hu, J. & Kivelson, S. A. Theory of electron nematic order in LaFeAsO. *Phys. Rev. B* **77,** 224509 (2008).
24. Kamiya, Y., Kawashima, N. & Batista, C. Dimensional crossover in the quasi-two-dimensional Ising-O(3) model. *Phys. Rev. B* **84,** 214429 (2011).
25. Avci, S. *et al.* Structural, magnetic, and superconducting properties of $Ba_{1-x}Na_xFe_2As_2$. *Phys. Rev. B* **88,** 094510 (2013).
26. Aswartham, S. *et al.* Hole doping in $BaFe_2As_2$: the case of $Ba_{1-x}Na_xFe_2As_2$ single crystals. *Phys. Rev. B* **85,** 224520 (2012).
27. Brydon, P. M. R., Schmiedt, J. & Timm, C. Microscopically derived Ginzburg-Landau theory for magnetic order in the iron pnictides. *Phys. Rev. B* **84,** 214510 (2011).
28. Giovannetti, G. *et al.* Proximity of iron pnictide superconductors to a quantum tricritical point. *Nat. Commun.* **2,** 398 (2011).
29. Kang, J. & Tešanović, Z. In *Proceedings of the March Meeting of the American Physical Society* (Dallas, TX, USA, 2013).
30. Hassinger, E. *et al.* Pressure-induced Fermi-surface reconstruction in the iron-arsenide superconductor $Ba_{1-x}K_xFe_2As_2$: Evidence of a phase transition inside the antiferromagnetic phase. *Phys. Rev. B* **86,** 140502(R) (2012).
31. Kim, M. *et al.* Antiferromagnetic ordering in the absence of structural distortion in $Ba(Fe_{1-x}Mn_x)_2As_2$. *Phys. Rev. B* **82,** 220503(R) (2010).
32. Avci, S. *et al.* Phase diagram of $Ba_{1-x}K_xFe_2As_2$. *Phys. Rev. B* **85,** 184507 (2012).
33. Avci, S. *et al.* Magnetoelastic coupling in the phase diagram of $Ba_{1-x}K_xFe_2As_2$ as seen via neutron diffraction. *Phys. Rev. B* **83,** 172503 (2011).
34. Nandi, S. *et al.* Anomalous suppression of the orthorhombic lattice distortion in superconducting $Ba(Fe_{1-x}Co_x)_2As_2$ single crystals. *Phys. Rev. Lett.* **104,** 057006 (2010).
35. Chubukov, A. V., Efremov, D. V. & Eremin, I. Magnetism, superconductivity, and pairing symmetry in iron-based superconductors. *Phys. Rev. B* **78,** 134512 (2008).
36. Fernandes, R. M. *et al.* Unconventional pairing in the iron arsenide superconductors. *Phys. Rev. B* **81,** 140501(R) (2010).

37. Vorontsov, A. B., Vavilov, M. G. & Chubukov, A. V. Superconductivity and spin-density waves in multiband metals. *Phys. Rev. B* **81,** 174538 (2010).

Acknowledgements

We are thankful to J. Knolle, R. Fernandes, J. Schmalian, R. Moessner and V. Stanev for useful discussions. This work was supported by the U.S. Department of Energy, Office of Science, Materials Sciences and Engineering Division (S.A., O.C., J.A., S.R., D.E.B., D.Y.C., M.G.K., J.-P.C., J.A.S., H.C., R.O.), which also supported A.V.C. under grant #DE-FG02-ER46900 (A.V.C.). I.E. acknowledges financial support from the DFG under priority programme SPP 1458 (ER 463/5) and the German Academic Exchange Service (DAAD PPP USA No. 57051534).

Author contributions

The neutron and x-ray diffraction experiments were devised by S.A., O.C., J.M.A., S.R. and R.O. and performed by S.A., O.C., J.M.A. and S.R. with experimental assistance from D.D.K., P.M. and A.D.A. The Rietveld refinements were performed by S.A. and O.C., with additional analysis by D.D.K. and J.M.A. The theoretical calculations were performed by I.E. and A.V.C. The samples were prepared by D.E.B., D.Y.C. and M.G.K. and characterized by J.P.C., J.A.S. and H.C. The manuscript was written by S.A., O.C., J.M.A., I.E., A.V.C. and R.O., and the Supplementary Information was written by J.M.A., I.E. and A.V.C.

Additional information

Supplementary Information accompanies this paper at http://www.nature.com/naturecommunications

Competing financial interests: The authors declare no competing financial interests.

Reprints and permission information is available online at http://www.npg.nature.com/reprintsandpermissions/

How to cite this article: Avci, S. *et al.* Magnetically driven suppression of nematic order in an iron-based superconductor. *Nat. Commun.* 5:3845 doi: 10.1038/ncomms4845 (2014).